Published in "Physical Review E 79(01): 016113, 2009"
which should be cited to refer to this work.

Predictive protocol of flocks with small-world connection pattern

Hai-Tao Zhang,[1,2] Michael Z. Q. Chen,[3,4,*] and Tao Zhou[5,6]

[1]*The Key Laboratory of Image Processing and Intelligent Control, Department of Control Science and Engineering, Huazhong University of Science and Technology, Wuhan 430074, People's Republic of China*

[2]*Department of Engineering, University of Cambridge, Cambridge CB2 1PZ, United Kingdom*

[3]*Department of Engineering, University of Leicester, Leicester LE1 7RH, United Kingdom*

[4]*Department of Electronic Engineering, City University of Hong Kong, Kowloon, Hong Kong SAR, People's Republic of China*

[5]*Department of Modern Physics, University of Science and Technology of China, Hefei 230026, People's Republic of China*

[6]*Department of Physics, University of Fribourg, Chemin du Muse 3, Fribourg CH-1700, Switzerland*

By introducing a predictive mechanism with small-world connections, we propose a new motion protocol for self-driven flocks. The small-world connections are implemented by randomly adding long-range interactions from the leader to a few distant agents, namely, pseudoleaders. The leader can directly affect the pseudoleaders, thereby influencing all the other agents through them efficiently. Moreover, these pseudoleaders are able to predict the leader's motion several steps ahead and use this information in decision making towards coherent flocking with more stable formation. It is shown that drastic improvement can be achieved in terms of both the consensus performance and the communication cost. From the engineering point of view, the current protocol allows for a significant improvement in the cohesion and rigidity of the formation at a fairly low cost of adding a few long-range links embedded with predictive capabilities. Significantly, this work uncovers an important feature of flocks that predictive capability and long-range links can compensate for the insufficiency of each other. These conclusions are valid for both the attractive and repulsive swarm model and the Vicsek model.

PACS number(s): 05.65.+b, 89.75.−k, 89.20.Kk

I. INTRODUCTION

Over the last decade, physicists have been looking for common, possibly universal, features of the collective behaviors of animals, bacteria, cells, molecular motors, as well as driven granular objects. The collective motion of a group of autonomous agents (or particles) is currently a subject of intensive research that has potential applications in biology, physics, and engineering. One of the most remarkable characteristics of systems, such as flocks of birds, schools of fish, and swarms of locusts, is the emergence of collective states in which the agents move in the same direction, i.e., an ordered state [1–7]. Moreover, this ordered state seeking problem for flocks, swarms, and schools can be further generalized to consensus [8], rendezvous, synchrony, cooperation, and so on. From the application aspect, this kind of distributed collective dynamic system has direct implications on sensor network data fusion, load balancing, unmanned air vehicles (UAVs), attitude alignment of satellite clusters, congestion control of communication networks, multiagent formation control, and global coordination for emergencies [9–12].

The interaction pattern of the natural biological flocks or swarms are neither entirely regular nor entirely random. An individual of a flock usually knows its neighbors, but its circle of interactions may not be confined to those nearby. In 1998, in order to describe the transition from a regular lattice to a random graph, Watts and Strogatz (WS) introduced the concept of the small-world network [13] by rewiring one end of a few connections to new nodes chosen at random from the whole network. With these few shortcuts, the average distance is decreased significantly without crucially changing the clustering property. The work on the WS small-world network has started an avalanche of research on complex networks. Especially, the synchronizability of networks can be greatly enhanced by introducing a few long-range connections [14–16]. Thus, for better synchronization in a flock of neighboring-connected agents with a leader, it is advantageous to build a small-world-type network structure by randomly adding long-range connections from the leader to a few distant agents (namely, *pseudoleaders*), so that the leader can affect them, thereby influencing all the other agents through them, via fast communication and rapid control commands.

Although a lot of relevant works were focused on network structures, recently, more and more researchers are interested in finding the rules of the interconnections present in abundant biogroups. Extraction of these rules can help interpret why the biogroups can demonstrate so many good characteristics such as synchronization, stabilization, and cohesion, amongst others. A fairly basic but popular flocking strategy is the Reynolds model [17], in which three elementary flocking protocols are prescribed: (i) *separation*: steer to avoid crowding and collision; (ii) *alignment*: steer towards the average heading; and (iii) *cohesion*: steer to move towards the average position. These rules have been proven effective and thus become the basic rules for the design of biogroup dynamic models. In 2003, Gazi and Passino [18] proposed an effective A/R (attractive or repulsive) swarm model in which the motion of each individual (autonomous agent or biological creature) is determined by two factors: (i) attraction to the

*Corresponding author: michael.chen@cantab.net

other individuals on long distances; and (ii) repulsion from the other individuals on short distances.

The Gazi and Passino A/R model [18], embedded with a similar mechanism of the intermolecular force, is derived from the biological flocks or swarms behaviors. Thus far, the general understanding is that the swarming behaviors result from an interplay between a long-range attraction and a short-range repulsion between the individuals [19,20]. In [9], Breder suggested a simple model composed of a constant attraction term and a repulsion term, which is inversely proportional to the square of the distance between two members, whereas in [20], Warburton and Lazarus studied the effects on cohesion of a family of attraction or repulsion functions. Moreover, in the physics community, a large volume of literature on systems with interactive particles has adopted functions of attractive and repulsive forces to investigate the dynamics of the system [21–27]. For instance, in [21,22], systems of particles interacting in a lattice are considered with attraction between particles located at different sites and repulsion between particles occupying the same site. It is discussed in [23] that, the structure of a nonuniform Lennard-Jones (LJ) liquid near a hard wall is approximated by a reference fluid with repulsive intermolecular forces in a self-consistently determined external mean field incorporating the effects of attractive forces.

With the A/R model [18], Gazi and Passino proved that the individuals will form a bounded cohesive swarm in a finite time. One year later, by adding another factor, i.e., attraction to the more favorable regions (or repulsion from the unfavorable regions), they generalized their former model into a social foraging swarm model [28]. Under suitable circumstances, agents in this modified model are apt to move to the more favorable regions. The A/R model has been adopted by physicists and biologists to model self-driven particles and biological flocks [4,29–34]. In 2004, Moreau [34] presented a linearized model of flocks, and proved that the flock is uniformly and globally cohesive to a bounded circle if and only if there exists an agent (the "leader") connecting to all other agents, directly or indirectly, over an arbitrary time interval. Other than these kinds of A/R models [18,28,34], another popular kind of model is that without leaders (i.e., homogeneous), where a very representative one is the Vicsek model [3]. In each step, every agent updates its velocity according to the average direction of its neighbors. With the decrease of external noise or the increase of the particle density, the collective behavior of the flock undergoes a phase transition from a disordered phase to an ordered phase with coherent movement directions. In 2003, Jadbabaie *et al.* [35] provided the convergence condition of the noise-free Vicsek model, i.e., there exists an infinite sequence of contiguous, nonempty, and bounded time intervals $[t_i, t_{i+1})$, starting at t_0=0, with the property that across each such interval, all the agents are connected together.

Although most of the previous works on flock dynamics yield many advantages such as synchronization, stabilization, cohesion, and quick consensus, agents within the networks only know the information currently available to them. In this paper, we highlight another appealing phenomenon, i.e., the universal existence of a predictive mechanism in various biological aggregated systems. A general physical

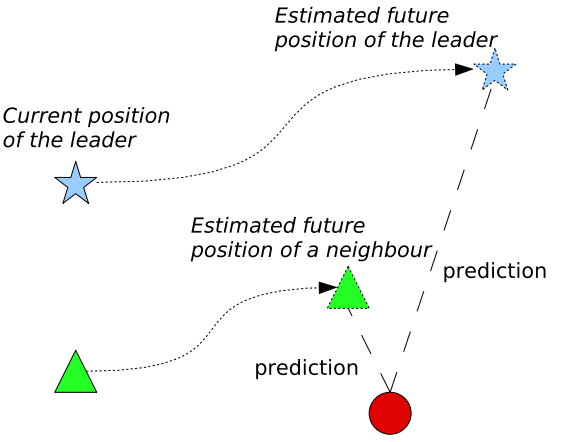

FIG. 1. (Color online) Predictive vision in natural biogroups. Each individual makes its motion decision based on not only the current status of the leader and its neighbors but also their future dynamics.

picture behind this is illustrated in Fig. 1 and interpreted as follows: in widely spread natural biogroups such as animals, bacteria, or cells, the decision on the next-step behavior of each individual is not solely based on the currently available state information (including position, velocity, etc.) of other (neighboring) agents inside the group but also on the predictions of future states. More precisely, taking a few past states of its leader and neighbors into account, an individual can estimate the corresponding future states several steps ahead and then make a decision.

Some experimental evidence has already been reported in the literature. In 1959, Woods [36] implemented some experiments on bee swarms and found a certain predictive mechanism of electronic signals inside this biogroup. Also for bee swarms, in 2002, Montague *et al.* [37] discovered that there exist some predictive protocols in the foraging process in uncertain environments. Apart from the investigation on the predictive mechanisms of swarming and foraging, other scholars focused on the predictive function of the optical and acoustical apparatuses of the individuals inside biogroups [38–40], especially cortexes and retinae. For instance, based on experiments on the bioeyesight systems, it was found that, when an individual observer prepared to follow a displacement of the stimulus with the eyes, visual form adaptation was transferred from current fixation to the future gaze position. These investigations strongly support our conjecture of the existence of some predictive mechanisms inside abundant biogroups.

Bearing in mind the plentiful examples of predictive protocols inside natural biogroups, we incorporated some predictive functions into a few long-range links, and found that it is possible to significantly enhance the flocking performances at a fairly low cost of the additional predictive energy. Furthermore, proper prediction capability can help reduce the minimal number of the long-range links between the leader and pseudoleaders, thus effectively decreasing the communication cost.

On the other hand, from the engineering application point of view, the phenomena and strategy reported in this paper may be applicable in relevant areas such as autonomous ro-

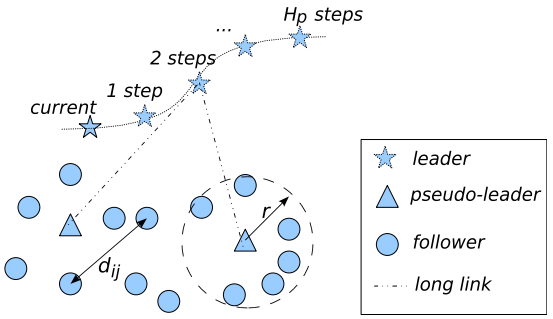

FIG. 2. (Color online) Small-world predictive mechanism of flocks. The leader (L), pseudoleaders (P), and followers (F) are denoted by stars, triangles, and circles, respectively, and the neighboring area of each individual is a circle with radius r centering at itself. The leader's trajectory is given in advance, which will not be influenced by the others. Each pseudoleader's dynamics is always influenced by both the leader's future position H_p steps ahead and its neighbors' positions, while each follower's dynamics is solely affected by its neighbors' positions.

bot formations, sensor networks, and UAVs [9,10,12]. Typically, due to the limitation of the communication energy, only a few agents have the capability to communicate with the leader. The incorporation of a predictive mechanism into these pseudoleaders can greatly improve the flocking performances.

The rest of the paper is organized as follows. In Sec. II, the small-world connection model with an embedded predictive mechanism is presented. Then, in Sec. III, its important role in improving flocking synchronization performances is extracted and analyzed by numerical simulations on the A/R model [18]. Afterwards, in Sec. IV, the generality of the virtues endowed by such a predictive mechanism is validated on the Vicsek model [3] as well. Finally, conclusions are drawn in Sec. V.

II. MODEL

It is well known that a ring-shaped network structure is not a good one for efficient mutual communication and global control within a flock of agents, while the so-called small-world networking structure performs much better. By adding a few long-range connections, the average path length of the ring-shaped network is abruptly decreased. This small-world effect is very desirable for fast communication and information transmission, efficient synchronization, and effective global control over the entire network [15]. Thus, in a flock of neighboring-connected agents with a leader, for communication and control purposes, it is advantageous to build a small-world-type network by randomly adding long-range connections from the leader to a few distant agents (namely, pseudoleaders). As shown in Fig. 2, the leader can affect pseudoleaders, thereby influencing all the other agents through them. To be clear, we call the nonspecial agents *followers*. Thus in our model, there are three different kinds of agents: leader (L), pseudoleaders (P), and followers (F).

In this model, the flock is assumed to move in an m-dimensional space and the standard A/R function [8,18,28]

$$G(d_{pL}) = -d_{pL}[a - b\exp(-\|d_{pL}\|_2^2/c)] \quad (1)$$

is used as long-range interaction from the leader (L) to each pseudoleader (P), where a, b, c are three free parameters, d_{pL} is the m-dimensional vector pointing from the predicted location of leader L to the current location of a pseudoleader p, and $\|d_{pL}\|_2 = \sqrt{d_{pL}^T d_{pL}}$ denotes the Euclidean distance between them. The force $G(d_{pL})$ is an m-dimensional vector whose direction is from the pseudoleader to the leader. For simplicity, in our model, the motion of the leader is given in advance, and will not be affected by any other agents. We assume that every pseudoleader has the same prediction horizon H_p, that is to say, a pseudoleader will predict the leader's location H_p steps ahead.

On the other hand, a weaker A/R function, representing the short-range interaction between two arbitrary neighboring agents i and j, is given as

$$g(d_{ij}) = -d_{ij}[\tilde{a} - \tilde{b}\exp(-\|d_{ij}\|_2^2/\tilde{c})], \quad (2)$$

where d_{ij} is the m-dimensional vector pointing from the individuals j to i, and $\|d_{ij}\|_2 = \sqrt{d_{ij}^T d_{ij}}$ denotes the Euclidean distance between them. The parameters $\tilde{a}$, $\tilde{b}$, and $\tilde{c}$ are much smaller than a, b, and c, respectively. The direction of vector $g(d_{ij})$ is from i to j. Denote by r the radius of the neighboring area (see Fig. 2). The neighboring A/R links could connect any two agents (F-F, P-P, and L-F) within the Euclidean distance r except the L-P interaction described in Eq. (1). Note that the leader can influence other agents, but will not be influenced. In order to decrease the prediction cost, no predictive mechanism is incorporated into the neighboring A/R links. Bearing in mind the physical meaning of the A/R function [8], the positions of a pseudoleader z_p and a fol-

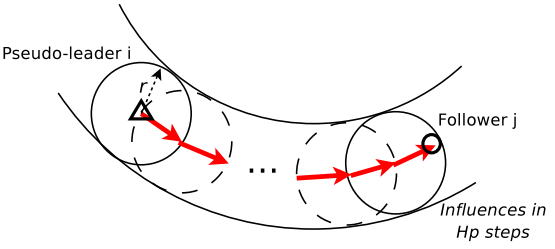

FIG. 3. (Color online) Information communication process inside flocks with a predictive mechanism. The arrows represent the passing of position information. If the pseudoleader i predicts the dynamics of the leader H_p steps ahead, then the follower j, within topological distance equaling H_p from i, could be affected by the current location of the leader. Here, an agent j has topological distance zero to itself, and 1 to all the agents located inside the circle with radius r centered on j. Two agents having topological distance 1 are called connected. An agent has topological distance D_T to j if and only if it is connected to at least one agent with distance $D_T - 1$ to j, and not connected with any agents having a distance smaller than $D_T - 1$ to j. Note that all the agents are not necessarily embedded in a circular pathway. Instead, due to the circle-shaped neighborhood of each agent, the position information transmission pathway forms a tube tangent to these neighboring circles, and the layout boundary of the pathway could be any type of curves depending on the location of the agents.

lower z_i (both z_p and z_i are m-dimensional vectors) are determined by

$$\dot{z}_p(t) = \underbrace{G[d_{pL}(t+H_p)]}_{\text{long link to the leader}} + \underbrace{\sum_{j\neq L, d_{pj}(t)\leqslant r} g[d_{pj}(t)]}_{\text{neighboring links}}, \quad (3)$$

and

$$\dot{z}_i(t) = \underbrace{\sum_{j, d_{ij}(t)\leqslant r} g[d_{ij}(t)]}_{\text{neighboring links}}, \quad (4)$$

respectively, where t denotes the current time, and $d_{pL}(t+H_p)$ represents the m-dimensional vector pointing from the leader's position H_p steps ahead to the current position of a pseudoleader. Although the rest of this paper concentrates on the motions in a two-dimensional space, the present model can be directly applied in any finite dimensional space. In this way, unlike the routine flocking strategies [18,28,34,41], a small-world interaction pattern is established with an embedded predictive mechanism, which has the capability of predicting the future behavior (position, velocity, etc.) of the leader several steps ahead. Note that (i) the structure of this interaction network will change in time since the location of each agent is varying; and (ii) in our simulations, the time label t is a discrete number with time step (or sampling interval) $T_s=1$, i.e., $\dot{x}(t)=[x(t+T_s)-x(t)]/T_s=x(t+1)-x(t)$.

The information communication process is illustrated in Fig. 3. The farthest agent i_1 directly communicating with agent i is among the ones at the rim of the circle with radius r centered on agent i. Analogously, the farthest agent i_2 directly influenced by i_1 is also located at the rim of the circle centered on agent i_1, and so forth. Finally, the influence of agent i reaches agent j in H_p steps. When agent j receives the information from agent i at time t, it is in fact a delayed information of agent i at time step $t-H_p$. However, if agent i acts as a pseudoleader who can accurately predict the behavior of the leader H_p steps ahead (i.e., the future dynamics at $t+H_p$), then, at time step t agent j's motion is affected by the exact current location of the leader $z_L(t)$ (i.e., the current dynamics at $t+H_p-H_p=t$). In this way, although agent j may not have a direct connection with the leader, it could know some information of the leader's current dynamics by agent i's delayed information. Therefore, agent j can adhere to the leader more tightly, making the flock's formation more likely to be rigid, and the coherence of the whole flock is thus improved effectively. Note that the predictive mechanism is valid only if the leader's motion is regular [42]. If the leader moves in some random, chaotic, or other irregular ways (e.g., a random walk), it is, in principle, impossible for the pseudoleaders to predict the leader's future location. Fortunately, in the real biological world, the flock leader always moves in some predictable pattern. Therefore, the other agents have the opportunity to display their predicting ability, such as that used by a chameleon to capture a fly or by a dog to catch a frisbee.

III. SIMULATION AND ANALYSIS

To show the advantages of the predictive mechanism, we compare the performances of the two cases of flocking with and without the predictive mechanism by simulations over an N-agent flock moving in a two-dimensional space. The

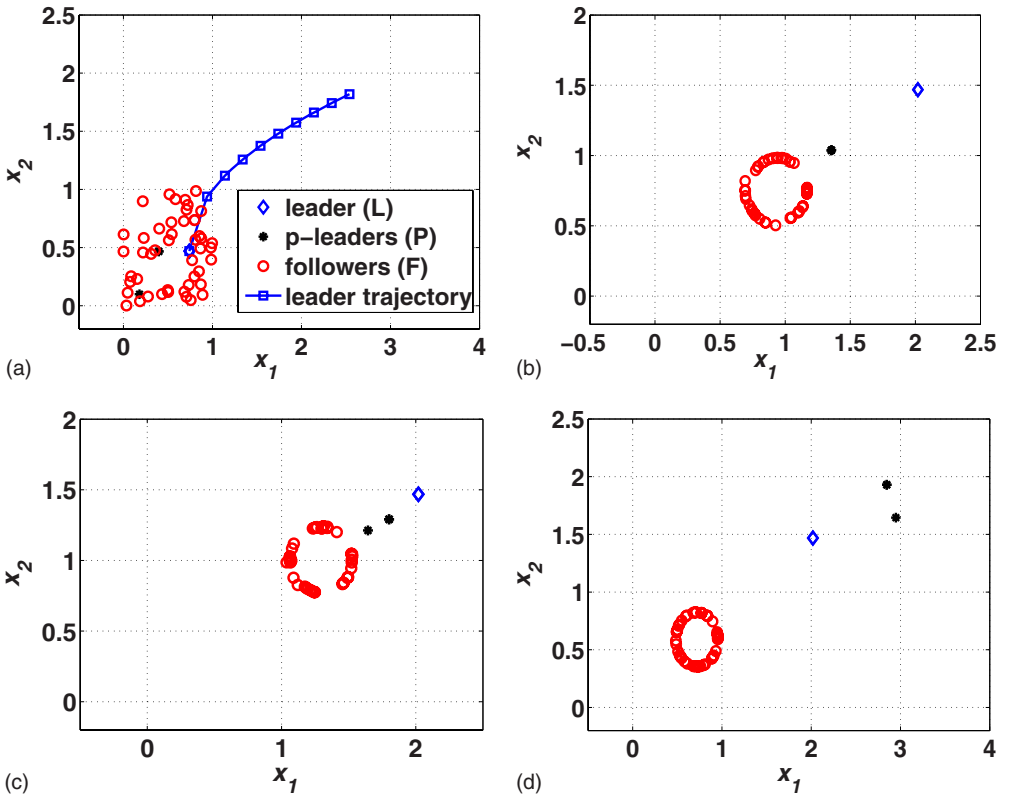

FIG. 4. (Color online) (a) Starting position of the 50-agent flock consisting of 1 leader, 2 pseudoleaders, and 47 followers. The blue line marked by square points denotes the trajectory of the leader. (b) Flock position after 65 steps without predictive mechanism ($H_p=0$), (c) with proper predictive mechanism ($H_p=20$), and (d) with overprediction ($H_p=70$). Here, x_1 and x_2 denote the two-dimensional position coordinates.

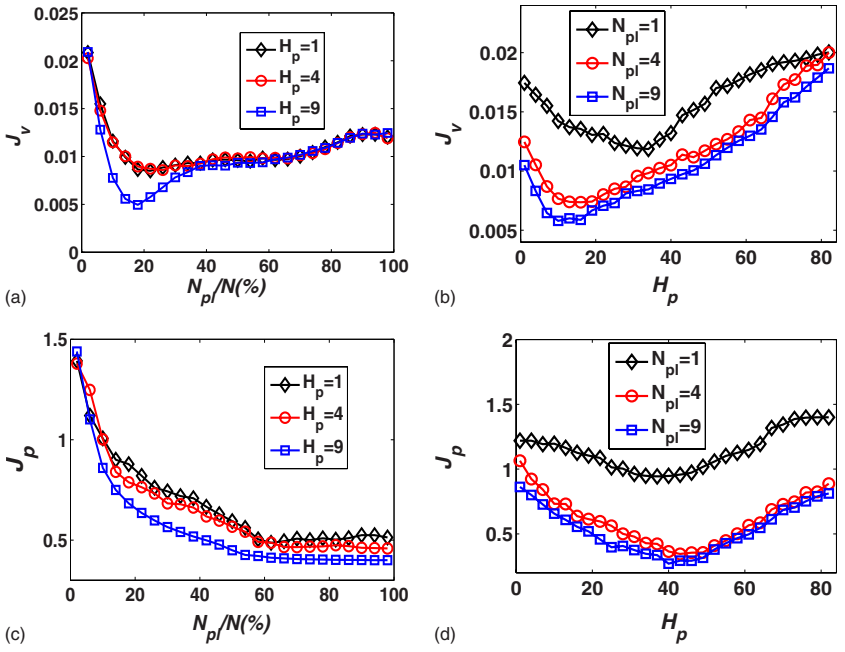

FIG. 5. (Color online) The roles of the pseudoleaders' number N_{pl} [(a) and (c)] and prediction horizon H_p [(b) and (d)] on a flock of 50 agents. The leader and the pseudoleaders are selected randomly among these agents. Each point is an average over 1000 independent runs. The parameters of the A/R functions (1) and (2) are $a=8$, $b=17.6$, $c=0.4$, and $\tilde{a}=1$, $\tilde{b}=2.2$, $\tilde{c}=0.2$, respectively. The radius of the influence circle is $r=0.65$. Each agent starts from a position randomly selected in the square $[0,1]\times[0,1]$. Without loss of generality, the trajectory of the leader is set along the curve defined by $x_2=\sqrt{x_1}$, and the velocity of the leader is $v_{L_{x_1}}(t)=0.02$, $v_{L_{x_2}}(t)=\sqrt{0.02(t+1)}-\sqrt{0.02t}$.

parameters are set as follows: the neighboring circle $r=0.65$, and the parameters of the A/R functions [see Eqs. (1) and (2)] of long-range links and neighboring links are set as $a=8$, $b=17.6$, $c=3.2$, and $\tilde{a}=1$, $\tilde{b}=2.2$, $\tilde{c}=0.2$, respectively. The former A/R function is much stronger in order to intensify the influence of the leader. As shown in Fig. 4(a), each agent starts from a position randomly selected in the square $[0,1]\times[0,1]$. The leader and pseudoleaders are selected randomly among these N agents. The trajectory of the leader is set as $x_2=\sqrt{x_1}$, and the velocity of the leader is $v_{L_{x_1}}(t)=0.02$, $v_{L_{x_2}}(t)=\sqrt{0.02(t+1)}-\sqrt{0.02t}$.

It can be seen from Figs. 4(b)–4(d) that, with a proper H_p, the coherence of the flock can be improved remarkably. The followers adhere to the leader much more tightly [see Fig. 4(c)], and the flock formation is more stable. More precisely, for the flocks with the predictive mechanism, the position error index

$$J_p=\frac{1}{N-1}\sum_{i=1,i\neq L}^{N}\|d_{iL}\|_2 \tag{5}$$

converges to a constant after finite steps, indicating a stable state of the flock dynamics. Here, J_p measures the cohesion performance of the flock, with $\|d_{iL}\|_2$ denoting the Euclidean distance between agent i (F or P) and the leader. Meanwhile, as to the flock without this mechanism, as shown in Fig. 4(b), J_p will keep increasing along with the elapse of time, making the flock unstable. However, abusing the foresight, namely, overprediction [see Fig. 4(d)], is also undesirable. That is because the pseudoleaders are attracted or repelled by the leader position too many steps ahead and will probably escape the flock with a fairly high speed, and then lose influence on the followers. In this way, the flocking will be damaged after finite steps.

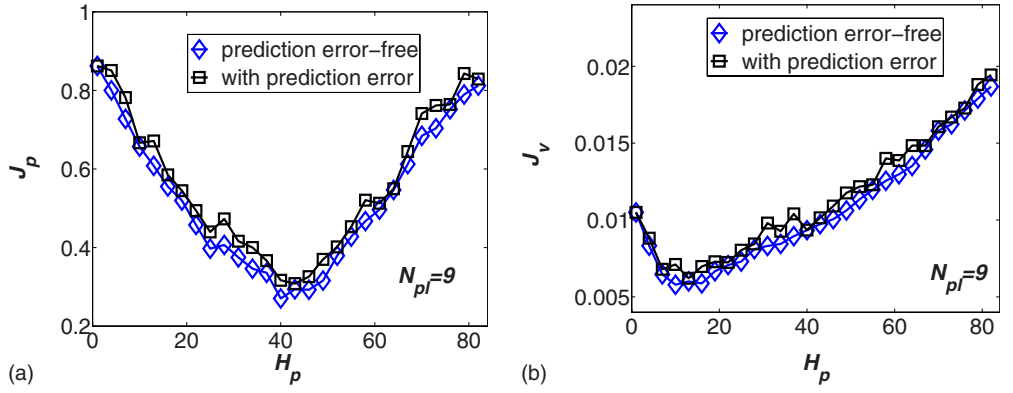

FIG. 6. (Color online) With-noise case vs. noise-free case for a flock with $N=50$, $N_{pl}=9$, and $\eta=0.02$. The other parameters and the initial conditions are the same as those in Fig. 5. Each point is an average over 1000 independent runs. The moderate external noise does not change the global behavior of the flock.

The circular formation of the followers in Figs. 4(b)–4(d) should be ascribed to the particular form of the A/R function. The biological flocking mechanisms are fairly complex, which can yield different kinds of collective behaviors. For example, fish use sidetrack to sense the current variances in which way the fish schools are formed. On the other hand, in order to save flying energy for the ones at the rear, wild geese flocks always form a "Λ"-like formation [43]. In this case, the forming process of such a flock is determined by aerodynamics. Our proposed model is based on the idea that an individual inside a biogroup can predict the trajectory of its leader(s), and this kind of intelligence can help the individual make a more efficient decision to improve the flocking performance. This paper, however, does not aim at reproducing the detailed movement formations of any particular biogroups.

In order to extract the role of H_p and the number of pseudoleaders denoted by N_{pl}, we display their influences on the position error index J_p and the velocity error index J_v in Fig. 5, where

$$J_v = \frac{1}{N-1}\sum_{i=1,i\neq L}^{N} \|\vec{v}_i - \vec{v}_L\|_2. \tag{6}$$

Here, J_v measures the formation performance of the flock, where $\vec{v}_L$ and $\vec{v}_i$ denote the velocity vectors of the leader and the ith agent (F or P). If $J_v \to 0$, the relative velocity of each pair of agents approaches zero, and thus the flock formation is fixed. In Fig. 5(a), we fix H_p and display the curves of J_v with increasing N_{pl}, while Fig. 5(b), on the contrary, reports the curves of J_v with increasing H_p and fixed N_{pl}. It can be seen from Fig. 5(a) that the curves fall quickly at the beginning and then more slowly until reaching a minimum, afterwards rising slowly with the increase of N_{pl}. It implies that adding just a proper number of pseudoleaders (e.g., long-range links) to the leader, which transforms the flock topology from a strongly localized network into a small-world one, will improve the flocking performance greatly. However, when the number of pseudoleaders reaches an optimum N_{pl}^* corresponding to the minimal J_v^*, the flock formation performance will start to worsen and these extra pseudoleaders become redundant. On the other hand, increasing H_p can help depress J_v with the same N_{pl}. Analogously, the J_v curves in Fig. 5(b) fall at the beginning until reaching the minimum, afterwards increasing all along and never reaching a stable platform. It implies that the flock formation performance can be remarkably improved with proper predictive capability. However, too much vision into the future, namely, overprediction, will even worsen the formation of flocking, which is consistent with what we have observed in Fig. 4(d). Besides, more pseudoleaders, i.e., larger N_{pl} (as long as $N_{pl} \leqslant N_{pl}^*$), can also help yield more cohesive flocking with better formation.

An interesting phenomenon can be observed from Fig. 5(a) that increasing pseudoleaders beyond some characteristic number makes the flocking performance worse, which seems counterintuitive. This can be explained as follows. If all the followers act as pseudoleaders, then they will align not to the current but to the future direction of the leader H_p steps ahead, which generally cannot yield optimal J_v. On the other hand, if N_{pl} is moderately decreased, then the increased followers lag behind the pseudoleaders and hence become more likely to align to the leader's current velocity via the tubelike information transmission as shown in Fig. 3. Therefore, the observation in Fig. 5(a) is reasonable. We give further discussions in Appendix A for interested readers.

Next, we investigate the effects of H_p and N_{pl} for another important index J_p. It can be seen from Fig. 5(c) that the

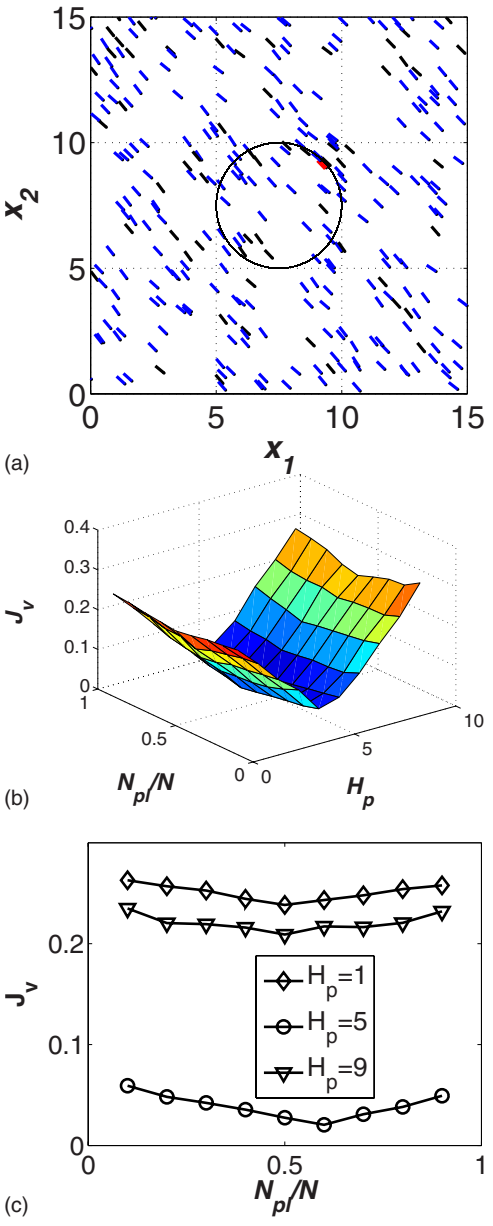

FIG. 7. (Color online) (a) Snapshot of the predictive Vicsek flock at the 12th running step. The red, black, and blue particles denote the leader, pseudoleaders, and followers, respectively. The centered black circle outlines the trajectory of the leader. In this case, the prediction horizon is H_p=4, and N_{pl}/N=20%. (b) Velocity synchronization index J_v as a function of the parameters H_p and N_{pl}. (c) The roles of N_{pl}/N on J_v. The parameters of this simulation are L=15, η=0.1, v=0.15, N=300, r=1, and $R=L/6$. The simulation result is averaged over 1500 independent runs.

curves fall sharply at the beginning and then asymptotically approach a stable value. The main difference between Figs. 5(a) and 5(c) is that the latter is monotonous and has no minimum, in other words, the increase of N_{pl} always improves J_p. A special case explaining this phenomenon is that, if all the followers serve as the pseudoleaders, then they will be very cohesive to the leader. However, this improvement on J_p also displays a saturation effect with increasing N_{pl}. On the other hand, compared with Fig. 5(c), the curves of Fig. 5(d) decrease more slowly first and then reach the lowest values at a fairly large H_p, and afterwards rise quickly. As a consequence, overprediction is not preferred. In brief, suitable insight into the future and moderate number of pseudoleaders are preferred.

A plausible physical rule behind the observed phenomena shown in Fig. 5 is that, in order to achieve a fixed flocking performance, greater predictive capability and more pseudoleaders can compensate the insufficiency of each other. Given a fixed-size flock, for formation performance J_v or cohesive performance J_p, there exists an optimized combination of H_p and N_{pl}. It is worth mentioning that the conclusions achieved in this paper are not sensitive to the trajectory of the leader. In order to validate the generality of the conclusions, we have also examined another two different trajectories, i.e., parabolic and sinusoidal curves. The simulation results are shown in Appendix B, which suggest that our main conclusion, i.e., predictive capability and long-range links can compensate for the insufficiency of each other, also holds in those two cases.

From a practical point of view, external perturbations (noise) and internal modeling mismatch are always present in any realistic system, which inevitably induces some prediction error for the pseudoleaders. To examine the influence of such prediction errors, we now introduce the perturbation into Eqs. (1) and (2) by adding an external two-dimensional white noise term $\xi \in [-\frac{1}{2}\eta, \frac{1}{2}\eta] \times [-\frac{1}{2}\eta, 1/2\,\eta]$ to the vector d_{pL}, i.e., $\hat{d}_{pL} = d_{pL} + \xi$ and $G(\hat{d}_{pL}) = -\hat{d}_{pL}[a - b\exp(-\|\hat{d}_{pL}\|_2^2/c)]$. The leader's position is no longer perfectly known to the pseudoleaders. From Fig. 6, one can observe that moderate external noises do not change the principal behavior of the flock, and hence the tendencies of the curves J_p and J_v are almost the same as the noise-free case. Furthermore, to understand deeply the capacity and robustness of our proposed predictive mechanism, we have also investigated the influences of stronger prediction errors ξ with other kinds of leader trajectories including the parabolic and sinusoidal curves in Appendix C. We found that the tolerance range of prediction error is large enough. The generality of the conclusions on the role of the predictive mechanism is thus further verified.

IV. PREDICTIVE MECHANISMS IN THE VICSEK MODEL

The role of predictive mechanisms highlighted in Sec. III is not merely confined to A/R flocks but is quite general. To verify this, we now incorporate this predictive mechanism into another well-accepted flocking model, i.e., the Vicsek model [3], and compare the synchronization performance of the predictive small-world Vicsek model with the one of the standard Vicsek model.

In this model, the velocities v_i of the N agents of the group are determined simultaneously at each discrete-time instant, and the position of the ith agent is updated as

$$x_i(k+1) = x_i(k) + v_i(k), \tag{7}$$

where $v_i(k)$ denotes the velocity vector of agent i at time k. The velocity $v_i(k)$ is characterized by a constant magnitude v and a direction $\theta_i(k)$ whose dynamics is given by

$$\theta_i(k+1) = \langle \theta_i(k) \rangle_r + \Delta\theta_i, \tag{8}$$

where $\langle \theta_i(k) \rangle_r$ denotes the average direction of all the agents' velocity vectors within a circle of radius r centered on agent i, i.e.,

$$\langle \theta_i(k) \rangle_r = \begin{cases} \arctan[\langle \sin(\theta_i(k)) \rangle_r / \langle \cos(\theta_i(k)) \rangle_r] & \text{if } \langle \cos(\theta_i(k)) \rangle_r \geqslant 0, \\ \arctan[\langle \sin(\theta_i(k)) \rangle_r / \langle \cos(\theta_i(k)) \rangle_r] + \pi & \text{otherwise}, \end{cases} \tag{9}$$

where $\langle \sin(\theta_i(k)) \rangle_r$ and $\langle \cos(\theta_i(k)) \rangle_r$ denote the average sine and cosine values, and $\Delta\theta_i$ represents a random noise obeying a uniform distribution in the interval $[-\eta/2, \eta/2]$.

As shown in Fig. 7(a) the particles are distributed in a square of dimension $[0, L] \times [0, L]$. The trajectory of the leader, which is not affected by others, is a circle centered at $(L/2, L/2)$ with radius $R = L/6$ so that the direction of the leader changes constantly. The small-world predictive connection framework shown in Fig. 2 is used together with the Vicsek model. Hence, the N_{pl} pseudoleaders are always influenced by the leader's velocity H_p steps ahead together with its neighbors' current velocities. It is shown in Figs. 7(b) and 7(c) that drastic improvement of the velocity synchronization performance can be achieved with moderate prediction horizons H_p and a suitable percentage of N_{pl}/N. Similar to the results of the A/R model shown in Sec. III, one can also conclude that suitable insight into the future and moderate number of pseudoleaders is preferable. Note that the Vicsek model aims at analyzing the direction consensus for self-driven particles [3], and it is less beneficial to investigate whether or not a more cohesive flock is better than a more evenly distributed one. Hence, we have solely focused on the velocity synchronization index J_v.

V. CONCLUSION AND DISCUSSION

Inspired by the predictive mechanisms that universally exist in abundant natural biogroups, we incorporate a certain predictive protocol into flocks with small-world structure. The predictive mechanism embedded in the pseudoleaders endows many neighboring-connected followers the capability of timely perceiving the current or even future dynamics of the leader, thus each individual can make a decision based on timely information of the leader instead of the delayed information as in some traditional models. In this way, the followers become more cohesive to the leader and the flock formation becomes more rigid. Note that, in our model, the leader's motion governs the trajectory of the whole swarm. However, it is a general feature of real migration flocks. In Ref. [41], a changeable target known by a few leaders is used to guide the whole flock, in which only the target's motion drives swarming behavior. Analogously, in this paper, a single leader is used to determine the general trajectory of the whole swarm. Therefore, the current leader-driven swarm is not unrealistic.

Simulation results led to the following conclusions: (i) Increasing the number of pseudoleaders can always improve the cohesive flocking performance. Furthermore, it can improve the formation flocking performance when the pseudoleader number has not exceeded a threshold, otherwise, the performance will be degraded. (ii) There exists a certain value of H_p that optimizes the cohesive and the formation flocking performances, in other words, moderately increasing H_p will improve the flocking performance, whereas overprediction will impair the flocking. (iii) Predictive capability and long-range links can compensate for the insufficiency of each other.

Furthermore, to verify the generality of these conclusions, we have also applied the predictive mechanism to another popular flock model, the directed graph model with linear dynamics [44,45]. The corresponding results also strongly suggest that predictive protocols are beneficial to flocking dynamics when taking both the flocking performance and the communication cost into consideration. More importantly, with this mechanism, only a very small proportion of the followers are required to act as the pseudoleaders to achieve a better flocking performance, as measured by J_p and J_v. From the engineering point of view, the value of this work is twofold: (i) The flocking performance is significantly improved by incorporation of a suitable predictive mechanism into the pseudoleaders. (ii) Moderately increasing the predictive capability can help remarkably decrease the required number of pseudoleaders. The latter feature is fairly useful for networks with insufficient long-range communication links, which are routinely costly.

This work provides a starting point aimed at achieving better flocking performance by using a predictive mechanism, and we hope that it will open new avenues in this fascinating direction.

ACKNOWLEDGMENTS

The authors would like to thank Professor Guanrong Chen, Professor Jan M. Maciejowski, and the anonymous referees for their valuable and constructive suggestions. H. T. Z. acknowledges the support of the National Natural Science Foundation of China (NNSFC) under Grant. No. 60704041, and financial support from The Research Fund for Doctoral Program (RFDP) under Grant No. 20070487090. M. Z. Q. C. acknowledges the support of the City University of Hong Kong under Grant No. 7002274. T. Z. acknowledges the support of the NNSFC under Grant No. 10635040.

APPENDIX A: SUPPLEMENTAL ILLUSTRATION OF FIG. 5(a)

To support our explanation, we have implemented new simulations on a small-scale flock with $N=4,5$, as shown in Fig. 8. The leader's trajectory is set as sinusoidal and circular curves in Figs. 8(a) and 8(b), respectively, so that the leader's direction changes continuously. It can be observed that, compared with the all-pseudoleader case [i.e., all the individuals act as pseudoleaders except the leader so that $N_{pl}=N-1$ (see the purple and red lines)], if only one pseudoleader is degraded into a follower (see the blue and black lines), J_v will be effectively decreased. Moreover, the improvement of J_v yielded by the single follower [see the red circle in Fig. 8(d)] is amplified by increasing H_p. The disadvantage of the all-pseudoleader case lies in the fact that all the $N-1$ pseudoleaders align to the leader's direction H_p steps ahead [see Fig. 8(c)] while, in the one-follower case, the single follower lagging behind the pseudoleaders is more likely to align to the current direction of the leader [see Fig. 8(d)], which effectively improves J_v. The reasonableness of our observation in Fig. 5(a) is thus verified.

APPENDIX B: EFFECTS OF THE PREDICTIVE MECHANISM WITH DIFFERENT LEADER'S TRAJECTORIES

The conclusions drawn in this paper are not sensitive to the leader's trajectory. In order to validate the generality of the conclusions on the role of predictive mechanisms, we have examined another two different trajectories, i.e., sinusoidal $[x_2=\sin(2x_1)+1]$ and parabolic $[x_2=x_1^2]$ curves. As shown in Figs. 9 and 10, regardless of the leader's trajectory, the influences of H_p and N_{pl} on the principal tendencies of both J_p and J_v remain the same. Those simulations suggest that our main conclusion, i.e., predictive capability and long-range links can compensate for the insufficiency of each other, is also valid in these two cases.

One may notice the difference between the optimal values of N_{pl}/N corresponding to the minimal J_v in Figs. 5(a) [or Fig. 10(a)] and 9(b). This should be due to the different kinds of leader trajectories. More precisely, the direction of the leader's sinusoidal trajectory [Fig. 9(a)] changes more intensively than that of Figs. 5(a) (square root curve) and 10(a) (parabolic curve), and hence a small proportion of pseudoleaders [such as 20% in Figs. 5(a) and 10(a)] cannot contain sufficient information to effectively guide the whole group. Therefore, more pseudoleaders [e.g., about 70% in Fig. 9(a)] are required to minimize J_v, and the optimal value of N_{pl}/N is remarkably higher in Fig. 9(a) than in Figs. 5(a)

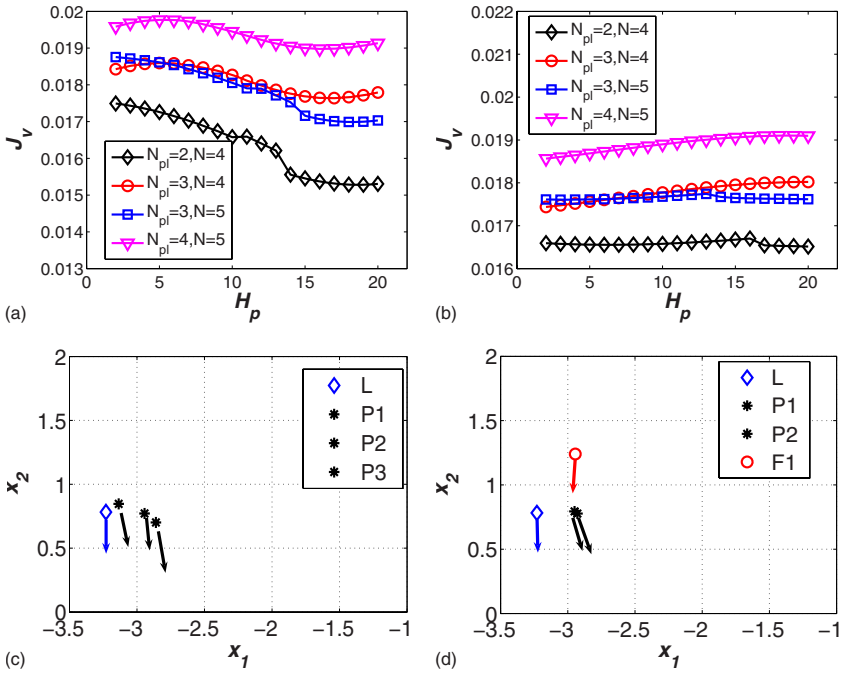

FIG. 8. (Color online) (a) Curve of J_v vs H_p with the leader's sinusoidal trajectory defined by $x_2=\sin(2x_1)+1$. (b) Curve of J_v vs H_p with the leader's circular trajectory defined by $(x_1+1.26)^2+(x_2-0.74)^2=4$. In both (a) and (b), each point is an average over 1000 independent runs. (c) Four-individual flock position and direction in the all-pseudoleader case. (d) Four-individual flock position and direction with only one follower (the red circle). Both (c) and (d) are snapshots at the 170th running step, with $H_p=15$ and the leader's circular trajectory given in (b).

and 10(a). Generally speaking, no matter what the leader's trajectory is, more pseudoleaders are not necessarily beneficial to J_v. It is worth mentioning that, as shown in Figs. 9(b) and 9(d), the oscillations of J_v and J_p along with increasing H_p are due to periodical changing of the position (in the x_2 dimension) and direction of the leader. In detail, although the followers may lag behind the current motion of the leader, J_v or J_p can also be improved if the followers happen to approach the leader's position (in the x_2 dimension) or velocity mT steps later. Here, T denotes the minimal period of the leader's trajectory, and m is an arbitrary positive integer.

APPENDIX C: EFFECTS OF PREDICTION ERRORS

In realistic system models, mismatch and external perturbations, which cause prediction errors, are always present. For completeness, we hereby examine the effects of the prediction errors on synchronization behavior of the flock. As shown in Fig. 11, we present curves of J_v and J_p with increasing noise magnitude $\eta=0,0.02,0.2,0.5$ for the cases of three different leader trajectories (square root, parabolic, and sinusoidal curves), respectively. It is observed that moderate prediction error ξ (e.g., $\xi\leqslant 0.2$) can hardly change the syn-

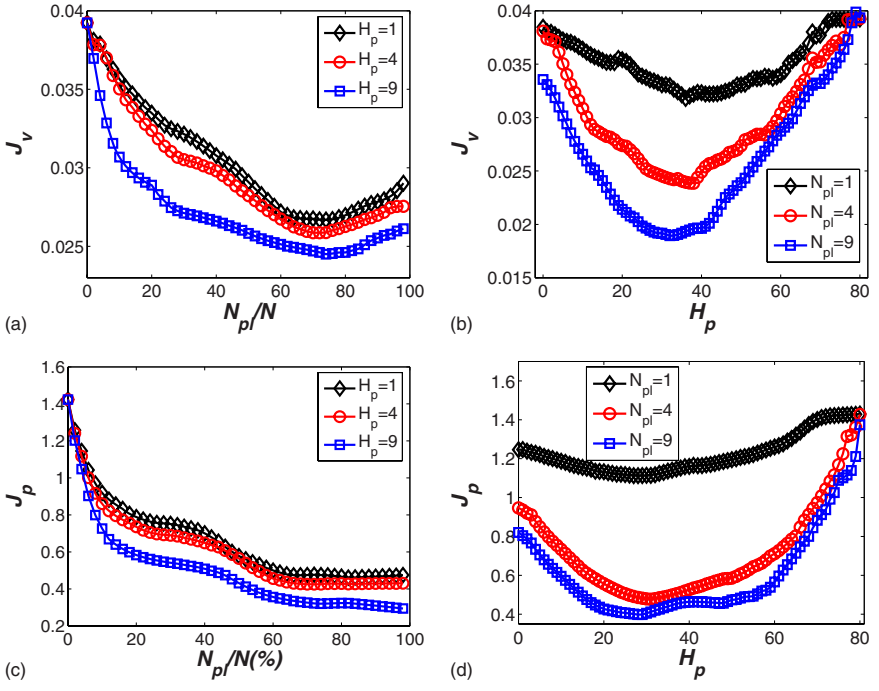

FIG. 9. (Color online) The roles of the pseudoleaders' number N_{pl} [(a) and (c)] and prediction horizon H_p [(b) and (d)] on a flock with a total of $N=50$ agents. The trajectory of the leader is set along the sinusoidal curve defined by $x_2=\sin(2x_1)+1$, and the velocity of the leader is $v_{L_{x_1}}(t)=0.02$, $v_{L_{x_2}}(t)=\sin[0.04(t+1)]-\sin(0.04t)$. The other parameters and initial conditions are the same as those in Fig. 5.

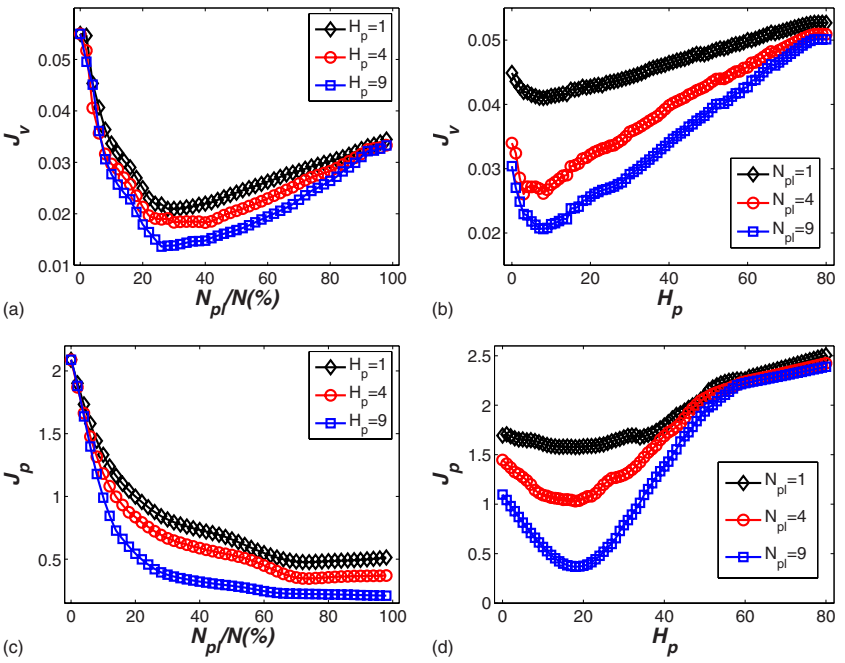

FIG. 10. (Color online) The roles of the pseudoleaders' number N_{pl} [(a) and (c)] and prediction horizon H_p [(b) and (d)] on a flock with a total of $N=50$ agents. The trajectory of the leader is set along the parabolic curve defined by $x_2=x_1^2$, and the velocity of the leader is $v_{L_{x_1}}(t)=0.02$, $v_{L_{x_2}}(t)=[0.02(t+1)]^2-(0.02t)^2$. The other parameters and initial conditions are the same as those in Fig. 5.

chronization tendency of the flock, which guarantees the feasibility and superiority of the current predictive mechanism. By comparison, too large ξ (e.g., $\xi \geqslant 0.5$) will inevitably impair the advantages of this predictive mechanism. This observation is reasonable since every method has its own limits and one cannot expect a poor prediction capability to yield a superb guidance for the flock. Fortunately, the tolerance range of prediction error is satisfactorily large, which further

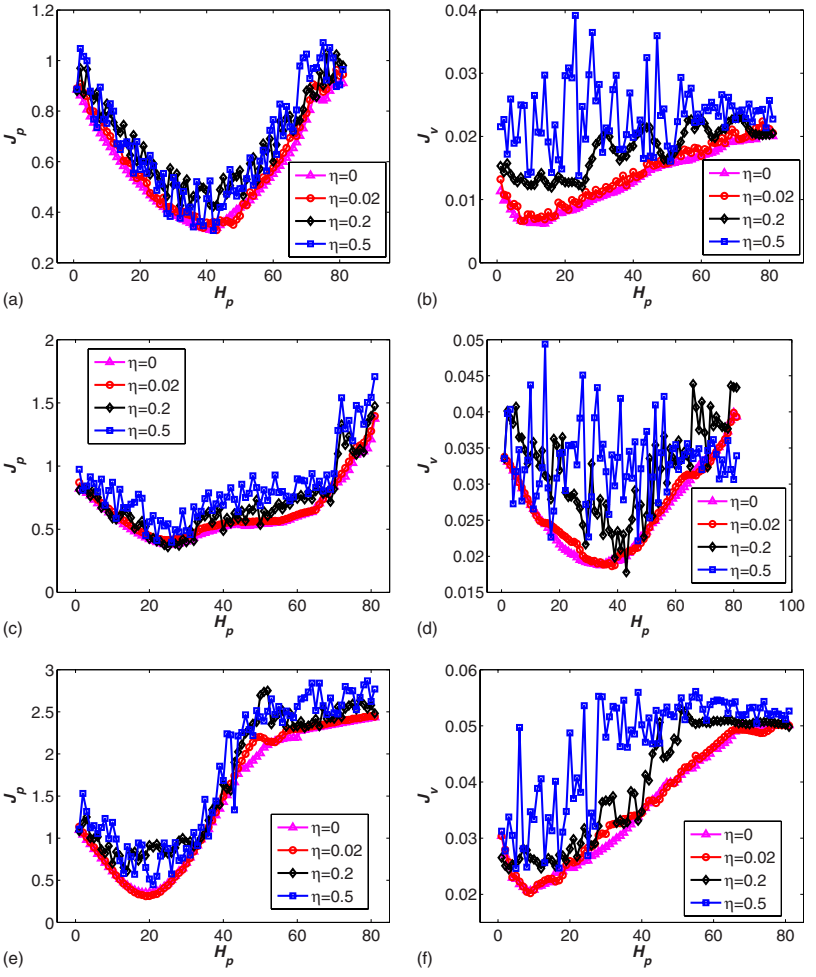

FIG. 11. (Color online) The effects of prediction error ξ. Here, the trajectory of the leader is set along the curve defined by $x_2=\sqrt{x_1}$ [(a) and (b)], $x_2=\sin(2x_1)+1$ [(c) and (d)] and $x_2=x_1^2$ [(e) and (f)], respectively. The flock size is $N=50$, and the number of pseudoleaders is $N_{pl}=9$. The other parameters and the initial conditions are the same as those in Fig. 5. Each point is averaged over 1000 independent runs. It can be found that moderate prediction error ξ does not change the principal behavior of the flock. If ξ, however, reaches a very large value, such as $\eta=0.5$, the benefits of prediction capability on J_v will almost vanish. Note that the curve of J_v is more sensitive than that of J_p, making the feasible prediction error range of J_v smaller than the counterpart of J_p.

verifies the generality of our proposed predictive mechanism. Note that the curve of J_p is more robust than the curve of J_v because the relative velocities are more easily deviated by prediction error than the relative positions.

[1] M. Aldana, V. Dossetti, C. Huepe, V. M. Kenkre, and H. Larralde, Phys. Rev. Lett. **98**, 095702 (2007).

[2] G. Grégoire and H. Chaté, Phys. Rev. Lett. **92**, 025702 (2004).

[3] T. Vicsek, A. Czirók, E. Ben-Jacob, I. Cohen, and O. Shochet, Phys. Rev. Lett. **75**, 1226 (1995).

[4] M. R. D'Orsogna, Y. L. Chuang, A. L. Bertozzi, and L. S. Chayes, Phys. Rev. Lett. **96**, 104302 (2006).

[5] H. Chaté, F. Ginelli, and R. Montagne, Phys. Rev. Lett. **96**, 180602 (2006).

[6] J. P. Hernandez-Ortiz, C. G. Stoltz, and M. D. Graham, Phys. Rev. Lett. **95**, 204501 (2005).

[7] W. Li, H. T. Zhang, M. Z. Q. Chen, and T. Zhou, Phys. Rev. E **77**, 021920 (2008).

[8] R. Olfati-Saber and R. Murray, IEEE Trans. Autom. Control **49**, 1520 (2004).

[9] I. F. Akyildiz, W. Su, Y. Sankarasubramaniam, and E. Cayirci, Comput. Netw. **38**, 393 (2002).

[10] T. Arai, E. Pagello, and L. E. Parker, IEEE Trans. Rob. Autom. **18**, 1292 (2002).

[11] D. Helbing, I. Farkas, and T. Vicsek, Nature (London) **407**, 487 (2000).

[12] P. Ogren, E. Fiorelli, and N. E. Leonard, IEEE Trans. Autom. Control **49**, 1292 (2004).

[13] D. J. Watts and S. H. Strogatz, Nature (London) **393**, 440 (1998).

[14] X. F. Wang and G. Chen, IEEE Trans. Circuits Syst., I: Fundam. Theory Appl. **49**, 54 (2002).

[15] T. Zhou, M. Zhao, and B. H. Wang, Phys. Rev. E **73**, 037101 (2006).

[16] M. Aldana and C. Huepe, J. Stat. Phys. **112**, 135 (2003).

[17] C. W. Reynolds, *Flocks, Herds, and Schools: A Distributed Behavioral Model, in Computer Graphics*, SIGGRAPH '87 Conference Proceedings, Vol. 21, pp. 25 (1987).

[18] V. Gazi and K. M. Passino, IEEE Trans. Autom. Control **48**, 692 (2003).

[19] C. M. Breder, Ecology **35**, 361 (1954).

[20] K. Warburton and J. Lazarus, J. Theor. Biol. **150**, 473 (1991).

[21] B. I. Lev, Phys. Rev. E **58**, R2681 (1998).

[22] E. D. Belotskii and B. I. Lev, Phys. Lett. A **147**, 13 (1990).

[23] J. D. Weeks, K. Katsov, and K. Vollmayr, Phys. Rev. Lett. **81**, 4400 (1998).

[24] A. J. Archer and N. B. Wilding, Phys. Rev. E **76**, 031501 (2007).

[25] P. Schlottmann, Phys. Rev. Lett. **68**, 1916 (1992).

[26] A. Melzer, V. A. Schweigert, and A. Piel, Phys. Rev. Lett. **83**, 3194 (1999).

[27] F. Ohnesorge and G. Binnig, Science **260**, 1451 (1993).

[28] V. Gazi and K. M. Passino, IEEE Trans. Syst., Man, Cybern., Part B: Cybern. **34**, 539 (2004).

[29] H. Shi, L. Wang, and T. Chu, Physica D **213**, 51 (2006).

[30] C. Zimmer, "From Ants to People: An Instinct to Swarm," *The New York Times*, November 13, 2007.

[31] Y. L. Chuang, M. R. D. Orsogna, D. Marthaler, A. L. Bertozzi, and L. S. Chayes, Physica D **232**, 33 (2007).

[32] X. Liu, J. Wang, and L. Huang, Physica A **386**, 543 (2007).

[33] X. Liu, J. Wang, and L. Huang, Physica A **383**, 733 (2007).

[34] L. Moreau, IEEE Trans. Autom. Control **50**, 169 (2005).

[35] A. Jadbabaie, J. Lin, and A. S. Morse, IEEE Trans. Autom. Control **48**, 988 (2003).

[36] E. F. Woods, Nature (London) **184**, 842 (1959).

[37] P. R. Montague, P. Dayan, C. Person, and T. J. Sejnowski, Nature (London) **377**, 725 (2002).

[38] J. A. Gottfried, J. O. Doherty, and R. J. Dolan, Science **301**, 1104 (2003).

[39] C. Summerfield, T. Egner, M. Greene, E. Koechlin, J. Mangles, and J. Hirsch, Science **314**, 1311 (2006).

[40] D. Melcher, Nat. Neurosci. **10**, 903 (2007).

[41] I. D. Couzin, J. Krause, N. R. Franks, and S. A. Levin, Nature (London) **433**, 513 (2005).

[42] In this paper, a trajectory is considered to be "regular" if it preserves a continuous, differentiable curve, like parabolic, sinusoidal and circular waves, along with the increasing time variable t. Moreover, it should not contain any large fluctuation or some chaoslike movement so that its future tendency can be predicted by smoothing the historical sequence. For instance, when catching a frisbee, a dog will make a prediction on its historical parabolic trajectory, and head for the predicted point. In this case, the trajectory of the frisbee is "regular," and this kind of example is easily available.

[43] J. Krause and G. D. Ruxton, *Living in Groups* (Oxford University Press, Oxford, 2002).

[44] H. T. Zhang, M. Z. Q. Chen, G. B. Stan, T. Zhou, and J. M. Maciejowski, IEEE Circuits Syst. Mag. **8** (3), 67 (2008).

[45] H. T. Zhang, M. Z. Q. Chen, T. Zhou, and G. B. Stan, Europhys. Lett. **83**, 40003 (2008).